JOINT TIME REVERSAL AND COMPRESSIVE SENSING BASED LOCALIZATION ALGORITHMS FOR MULTIPLE-INPUT MULTIPLE-OUTPUT RADARS

Mohammad H. S. Sajjadieh[†] *and Amir Asif*[‡]

[†]Electrical Engineering and Computer Science, York University, Toronto, ON, Canada M3J 1P3
[‡]Electrical and Computer Engineering, Concordia University, Montreal, QC, Canada H3J 1P8

ABSTRACT

The source localization problem for multiple-input, multiple-output (MIMO) radars was recently formulated by Yu et al. [7] in the compressive sensing (CS) framework. The resulting CS/MIMO radar achieves high resolution in joint direction and Doppler estimation, which is more pronounced with sparse data. However, the CS/MIMO technology does not operate well in environments with multipath, as is the case for low-angle targets located over flat surfaces. The paper applies the principle of time reversal (TR) to the CS/MIMO radar to converge the TR probing signal on the target leading to a stronger backscatter from the target as compared to the ones received from surrounding clutter. Monte Carlo simulations verify the superiority of the CSTR/MIMO radar over its CS/MIMO version without TR.

***Index Terms*—** Compressive sensing, Source localization, Direction of arrival, Doppler estimation, MIMO radar, Time reversal.

1. INTRODUCTION

Unlike standard phased array radars, multiple-input multiple-output (MIMO) radars [1]-[20] transmit simultaneous probing signals from all elements of the MIMO array, which can be quite different from each other. The resulting MIMO diversity is then exploited by the localization technology for a much superior system-wide performance. Based on how the constituent arrays are configured, MIMO radars are classified into two categories: (1) Multistatic MIMO radars with spatially distributed transmit and receive elements designed to provide spatial diversity by viewing the target from different angles, and; (2) Colocated MIMO radars with transmit and receive antennas in close proximity to cohere a beam towards a certain direction in space. The paper focuses on the colocated MIMO setup that takes advantage of waveform diversity [19] to offer improvements in angular resolution, enhanced parameter identifiability, and increased flexibility in transmit/receive beampattern design. A major problem with colocated MIMO radars is the large amount of data generated at the receive elements due to the high sampling rate used to digitize the backscatter observations from the target. This places considerable computational power, storage, and bandwidth requirements on the MIMO system. The application of compressive sampling (CS) to a colocated MIMO radar was recently investigated in [7], where each receive node applies CS to its received signal to reduce the number of recorded samples. Using the CS formulation, Poor et al. [7] expressed the estimation of the parameters (e.g., direction of arrival (DOA), and Doppler shift associated with L targets) from the recorded $(N_s \times 1)$ signal vector $\mathbf{x}$ as the ℓ_1-optimization problem

$$\min \|\mathbf{s}\|_1, \qquad \text{such that (s.t.)} \quad \mathbf{r}_c = \mathbf{\Phi x} = \mathbf{\Phi \Psi s}, \tag{1}$$

where $\mathbf{s}$ is a sparse vector with K nonzero elements representing L targets. CS makes use of the fact that the backscatter observation $\mathbf{x}$ reflected from the targets is sparse in at least one domain. Expressed in terms of the proper basis $\mathbf{\Psi}$, $\mathbf{x}$, therefore, has a concise representation $\mathbf{s}$. Referred to as the CS dictionary, the columns of $\mathbf{\Psi}$ are called atoms and are typically orthogonal or near-orthogonal to each other. The number of samples in $\mathbf{x}$ is further reduced by multiplying $\mathbf{x}$ with a $(N_c \times N_s)$ random orthogonal compressive matrix $\mathbf{\Phi}$ that is incoherent with $\mathbf{\Psi}$. The angle-Doppler estimation problem in the CS/MIMO radar, therefore, uses CS, Eq. (1), to solve for the parameter vector $\mathbf{s}$ given sparse observations $\mathbf{r}_c$ (with length $N_c \ll N_s$) from all receive elements available at the fusion center.

A necessary condition for the aforementioned CS approach is channel sparsity, which is automatically satisfied when relative to the number of available snapshots, the number of targets is small. In channels with strong multipath, the number K of nonzero elements in $\mathbf{s}$ increases as each additional path introduces its own set of unknown localization parameters. Multipath, therefore, has a detrimental effect on the performance of the CS/MIMO radar. In the best case scenario, multipath increases the complexity of the CS step in the CS/MIMO radar. In the worst case, there is a potential for the sparsity condition to be violated even with few targets present. In our previous work, we have applied the time-reversal (TR) principle to multiple-scattering medium, where explicit modeling of the medium is difficult due to its complexity or due to random perturbations. In this paper, we couple TR to the CS/MIMO radar to propose the compressive sensing, TR MIMO (CSTR/MIMO) radar that includes an additional TR stage. In the CSTR/MIMO radar, the previously recorded CS/MIMO backscatter is time reversed, energy normalized, and retransmitted into the medium. As the process is repeated, the TR signal becomes highly focused on the targets producing stronger backscatter reflections from the targets compared to those from the clutter. Consequently, the energy in the recorded backscatter is redistributed in favour of the reflections from the targets. To assess the potential of applying TR, our simulations operate both radars with 12.5% of the raw samples using CS, i.e., $N_c = 0.125N_s$.

Section 2 formulates the signal model for the MIMO radar operating in strong multipath. In Section 3, the CS based approach for the joint estimation of the Doppler shift, direction of departure (DOD), and DOA in the CS/MIMO system (without TR) is presented. In Section 4, we derive the signal model for the CSTR/MIMO radar followed by its estimation algorithm in Section 5. The performance of CSTR/MIMO and CS/MIMO radars is compared in Section 6 using Monte Carlo simulations. Finally, Section 7 concludes the paper.

2. MIMO SYSTEM FORMULATION IN MULTIPATH

Consider the MIMO radar with two sets of transceivers $\mathcal{A}$ and $\mathcal{B}$. A set of N_t transmit elements in transceiver $\mathcal{A}$ is used to probe the channel, while a second set of N_r receive elements in transceiver $\mathcal{B}$

records the backscatter. All N_t transmit elements simultaneously probe the channel with the probing signal $f_i(t)e^{\jmath\omega_c t}$, where $f_i(t)$ is the baseband waveform associated with transmit element i, $(1 \le i \le N_t)$, and ω_c is the carrier frequency. The signal recorded at the receive elements is the accumulative backscatter from L targets and $(M_f - L)$ scatterers representing clutter. In the forward direction, the signal incident on scatterer m_f, $(1 \le m_f \le M_f)$, is given by

$$s_{m_f}(t) = \sum_{i=1}^{N_t} \alpha_{m_f} f_i\left(t - \tau_{(i,m_f)}(t)\right) e^{\jmath\omega_c\left(t-\tau_{(i,m_f)}(t)\right)}, \quad (2)$$

where α_{m_f}, $\tau_{(i,m_f)}$ and θ_{m_f} are, respectively, the attenuation, delay, and direction of departure (DOD) associated with the forward path to scatterer m_f. Expressed in terms of the reference delay $\tau_{m_f}(0)$ between the reference transmit element and scatterer m_f, delay $\tau_{(i,m_f)}$ for transmit element i is expressed as

$$\tau_{(i,m_f)}(t) = \tau_{m_f}(0) + \frac{v_{m_f}}{c}t + \tau_i(\theta_{m_f}), \quad (3)$$

where v_{m_f} is the relative velocity of scatterer m_f, c is the wave propagation speed, and $\tau_i(\theta_{m_f}) = d_i \sin(\theta_{m_f})/c$ is the delay associated with scatterer m_f in addition to $\tau_{m_f}(0)$, which depends upon interelement spacing d_i between transmit element i and reference element. The observation at receive element j, $(1 \le j \le N_r)$, is the accumulation of the line-of-sight backscatters from all scatterers as well as the backscatters reaching the receive element after multiple reflections between different scatterers. With a total of M_b paths in the back propagation model, the observation at receive element j is given by

$$r_j(t) = \sum_{m_b=1}^{M_b} \alpha_{m_b} \sum_{m_f=1}^{M_f} s_{m_f}\left(t - \tau_{(j,m_b)}(t)\right) + n''_j(t), \quad (4)$$

where $n''_j(t)$ is the observation noise , α_{m_b} is the attenuation for backward path m_b. As for the forward path, the delay $\tau_{(j,m_b)}(t)$ for backward path m_b is given by

$$\tau_{(j,m_b)}(t) = \tau_{m_b}(0) + \frac{v_{m_b}}{c}t + \tau_j(\theta_{m_b}), \quad (5)$$

where $\tau_{m_b}(0)$, v_{m_b}, and $\tau_i(\theta_{m_b})$ are range delay, velocity, and direction DOA for backward path m_b with respect tot the reference element in the receive array. The DOA $\tau_j(\theta_{m_b}) = d_j \sin(\theta_{m_b})/c$, where d_j the distance between receive element j and reference element in array $\mathcal{B}$. Substituting $s_{m_f}(t)$ from Eq. (2) in Eq. (4) yields

$$r_j(t) = \sum_{i}^{N_t}\sum_{m_b}^{M_b}\sum_{m_f}^{M_f} \alpha_{m_f}\alpha_{m_b} e^{\jmath\omega_c\left(t-\left(\tau_{(i,m_f)}(t)+\tau_{(j,m_b)}(t)\right)\right)} \quad (6)$$
$$\times f_i\left(t - \left(\tau_{(i,m_f)}(t) + \tau_{(j,m_b)}(t)\right)\right) + n''_j(t).$$

Demodulating (6) and considering $f_i(t)$ as a narrowband probe gives

$$r_j(t) = \sum_{i}^{N_t}\sum_{m_b}^{M_b}\sum_{m_f}^{M_f} \alpha_{m_f}\alpha_{m_b} f_i(t) e^{-\jmath\omega_c\left(\tau_{(i,m_f)}(t)+\tau_{(j,m_b)}(t)\right)} + n'_j(t), \quad (7)$$

where $n'_j(t)$ is an additive white Gaussian noise with the PSD of σ'^2_j. Inserting Eq. (3) and Eq. (5) into Eq. (7) yields

$$r_j(t) = \sum_{i}^{N_t}\sum_{m_b}^{M_b}\sum_{m_f}^{M_f} \left(\alpha_{m_f}\alpha_{m_b} e^{-\jmath\omega_c\left(\tau_{m_f}(0)+\tau_{m_b}(0)\right)}\right) \times \quad (8)$$
$$e^{-\jmath\omega_c\left(\beta_{m_f}+\beta_{m_b}\right)t} \cdot e^{-\jmath\omega_c\left(\tau_i(\theta_{m_f})+\tau_j(\theta_{m_b})\right)} f_i(t) + n'_j(t),$$

where $\beta_{m_f} = -\jmath\omega_c v_{m_f}/c$ and $\beta_{m_f} = -\jmath\omega_c v_{m_b}/c$ are forward and backward Doppler shifts, respectively. By combining the forward and backward propagation paths into $(1 \le l = (m_f, m_b) \le L)$ complete paths between the transmit and receive elements, Eq. (8) is expressed in the vector-matrix format as

$$r_j(t) = \sum_{l=1}^{L} \alpha_l d(t, \beta_l)\mathbf{f}^T(t)\mathbf{v}(j, \tau(\theta_l)) + n'_j(t), \quad (9)$$

where

$$\alpha_l = \alpha_{m_f}\alpha_{m_b} e^{-\jmath\omega_c(\tau_{m_f}(0)+\tau_{m_b}(0))}, d(t,\beta_l) = e^{-\jmath\omega_c(\beta_{m_f}+\beta_{m_b})t},$$
$$\boldsymbol{\theta}_l = (\theta_{m_f}, \theta_{m_b}), \beta_l = \beta_{m_f} + \beta_{m_b}, \mathbf{f}(t) = [f_1(t), \cdots, f_N(t)]^T,$$
$$\text{and } \mathbf{v}(j, \tau(\boldsymbol{\theta}_l)) = \Big[e^{-\jmath\omega_c\left(\tau_1(\theta_{m_f})+\tau_j(\theta_{m_b})\right)}, \cdots, e^{-\jmath\omega_c\left(\tau_{N_t}(\theta_{m_f})+\tau_j(\theta_{m_b})\right)}\Big]^T,$$

where T as superscript denotes the transcript operator. In MIMO radars, the probing signals $\{f_i(t)\}$ typically consist of a sequence of pulses with a constant pulse repetition interval (PRI). For a total of N_p pulses with the PRI of T_p, sampling period denoted by T_s, and number of samples in each pulse, $(1 \le p \le N_p)$, given by N_s, the response to pulse p in Eq. (9) is discretized and given by

$$\mathbf{r}_{(j,p)} = [r_j((p-1)T+0T_s), \cdots, r_j((p-1)T+(N_s-1)T_s)]^T \quad (10)$$
$$= \sum_{l=1}^{L} \alpha_l d((p-1)T, \beta_l)\mathbf{D}(\beta_l)\mathbf{F}(t)\mathbf{v}(j, \tau(\boldsymbol{\theta}_l)) + \mathbf{n}'_{(j,p)},$$
$$\text{where } \mathbf{D}(\beta_l) = \text{diag}\left\{\left[e^{-\jmath\omega_c\beta_l(0)T_s}, \cdots, e^{-\jmath\omega_c\beta_l(N_s-1)T_s}\right]\right\},$$
$$\mathbf{F}(t) = [\mathbf{f}(0T_s), \cdots, \mathbf{f}((N_s-1)T_s)]^T,$$
$$\text{and } \mathbf{n}'_{(j,p)} = \left[n'_j((p-1)T + (0)T_s), \cdots, n'_j((p-1)T + (N_s-1)T_s)\right]^T.$$

In the following derivation, the DOD and DOA are treated separately as given by $\boldsymbol{\theta}_l = (\theta_{m_f}, \theta_{m_b})$, while the Doppler shifts associated with the forward and backward signal propagations $\{\beta_{m_f}, \beta_{m_b}\}$ for the same target are added together and treated as one variable β_l as is customary in array processing.

3. THE CS/MIMO RADAR

Following [7], we discretize the channel into an angle-Doppler plane with L' cells as $\mathbf{a} = [(\boldsymbol{\theta}_1, \beta_1), \cdots, (\boldsymbol{\theta}_{L'}, \beta_{L'})]$ and define a dictionary for transceiver j and pulse p as

$$\boldsymbol{\Psi}^{(\mathrm{C})}_{(j,p)}(\mathbf{a}) \triangleq [d((p-1)T, \beta_1)\mathbf{D}(\beta_1)\mathbf{F}(t)\mathbf{v}(j, \tau(\boldsymbol{\theta}_1)), \cdots, \quad (11)$$
$$d((p-1)T, \beta_{L'})\mathbf{D}(\beta_{L'})\mathbf{F}(t)\mathbf{v}(j, \tau(\boldsymbol{\theta}_{L'}))].$$

Considering the received signal at the jth transceiver in Eq. (10) and the dictionary defined in Eq. (11), we construct a vector of unknowns $\mathbf{s}^{(\mathrm{C})}_{(j,p)} = [\alpha_1, \cdots, \alpha_{L'}]^T$. In terms of $\mathbf{s}^{(\mathrm{C})}_{(j,p)}$, Eq. (10) is expressed in the matrix-vector format as

$$\mathbf{r}_{(j,p)} = \boldsymbol{\Psi}^{(\mathrm{C})}_{(j,p)}(\mathbf{a})\mathbf{s}^{(\mathrm{C})}_{(j,p)} + \mathbf{n}'_{(j,p)}. \quad (12)$$

The compressed version of $\mathbf{r}_{(j,p)}$ is produced by multiplying it with a $(N_c \times N_s)$ zero-mean Gaussian matrix $\boldsymbol{\Phi}^{(\mathrm{C})}_{(j,p)}$, with $(N_c < N_s)$, and is given by

$$\mathbf{r}_{c(j,p)} = \boldsymbol{\Phi}^{(\mathrm{C})}_{(j,p)}\boldsymbol{\Psi}^{(\mathrm{C})}_{(j,p)}(\mathbf{a})\mathbf{s}^{(\mathrm{C})}_{(j,p)} + \mathbf{n}_{(j,p)}, \quad (13)$$

with $\mathbf{n}_{(j,p)}$ the downsampled version of noise $\mathbf{n}'_{(j,p)}$ to keep it consistent in dimensions with $\mathbf{r}_{c(j,p)}$. At the fusion center, combining all pulses from all N_r receive elements gives

$$\begin{aligned}\mathbf{r}_c &= \left[\mathbf{r}^T_{c(1,1)}, \cdots, \mathbf{r}^T_{c(1,N_p)}, \cdots, \mathbf{r}^T_{c(N_r,1)}, \cdots, \mathbf{r}^T_{c(N_r,N_p)}\right]^T \\ &= \mathbf{\Theta}^{(\mathrm{C})}_{r_c}\mathbf{s}^{(\mathrm{C})} + \hat{\mathbf{n}},\end{aligned} \tag{14}$$

where $\mathbf{\Theta}^{(\mathrm{C})}_{r_c} = \Big[\Big(\mathbf{\Phi}^{(\mathrm{C})}_{(1,1)}\mathbf{\Psi}^{(\mathrm{C})}_{(1,1)}\Big)^T, \cdots, \Big(\mathbf{\Phi}^{(\mathrm{C})}_{(1,N_p)}\mathbf{\Psi}^{(\mathrm{C})}_{(1,N_p)}\Big)^T,$

$\cdots, \Big(\mathbf{\Phi}^{(\mathrm{C})}_{(N_r,1)}\mathbf{\Psi}^{(\mathrm{C})}_{(N_r,1)}\Big)^T, \cdots, \Big(\mathbf{\Phi}^{(\mathrm{C})}_{(N_r,N_p)}\mathbf{\Psi}^{(\mathrm{C})}_{(N_r,N_p)}\Big)^T\Big]^T$

and $\hat{\mathbf{n}} = \Big[\Big(\mathbf{\Phi}^{(\mathrm{C})}_{(1,1)}\mathbf{n}'_{(1,1)}\Big)^T, \cdots, \Big(\mathbf{\Phi}^{(\mathrm{C})}_{(1,N_p)}\mathbf{n}'_{(1,N_p)}\Big)^T,$

$\cdots, \Big(\mathbf{\Phi}^{(\mathrm{C})}_{(N_r,1)}\mathbf{n}'_{(N_r,1)}\Big)^T, \cdots, \Big(\mathbf{\Phi}^{(\mathrm{C})}_{(N_r,N_p)}\mathbf{n}'_{(N_r,N_p)}\Big)^T\Big]^T.$

The fusion center recovers $\mathbf{s}^{(\mathrm{C})}$ in Eq. (14) using the Dantzig selector [21] given below

$$\hat{\mathbf{s}}^{(\mathrm{C})} = \min \left\|\mathbf{s}^{(\mathrm{C})}\right\|_1 \text{ s.t. } \left\|(\mathbf{\Theta}^{(\mathrm{C})}_{r_c})^H(\mathbf{r}_c - \mathbf{\Theta}^{(\mathrm{C})}_{r_c}\mathbf{s}^{(\mathrm{C})})\right\|_\infty < \mu^{(\mathrm{C})}. \tag{15}$$

To ensure that the columns of the sensing matrix $\mathbf{\Theta}_{r_c}$ are approximately orthogonal, a high number $\{N_t, N_r\}$ of transceiver elements and a high number of pulses N_p are needed. Further, the value of $\mu^{(\mathrm{C})}$ depends on the maximum norm for the columns of the sensing matrix $\mathbf{\Theta}^{(\mathrm{C})}_{r_c}$ and variance of noise $\hat{\mathbf{n}}$. In [7], authors suggest $\mu^{(\mathrm{C})} < \left\|(\mathbf{\Theta}^{(\mathrm{C})}_{r_c})^H\mathbf{r}_c\right\|_\infty$.

4. TR MIMO RADAR FORMULATION IN MULTIPATH

In TR, [22]-[32] all receive elements time reverse, normalize their observations by factor $g_j = \sqrt{\|\mathbf{F}\|_2 / \|\mathbf{r}_j\|_2}$ and retransmit the resulting signals into the channel. The TR observation [31] made at transmit element k, $(1 \le k \le N_r)$, is given by

$$\begin{aligned}z_k(t) = &\sum_j^{N_r} g_j \sum_i^{N_t}\sum_{m'_b}^{M'_b}\sum_{m'_f}^{M'_f}\sum_{m_b}^{M_b}\sum_{m_f}^{M_f}(\overbrace{\alpha_{m'_f}\alpha_{m'_b}}^{A}\alpha_{m_f}\alpha_{m_b}) \\ &\times e^{-\jmath\omega_c(\overbrace{\tau_{m'_f}(0)+\tau_{m'_b}(0)}^{B}+\tau_{m_f}(0)+\tau_{m_b}(0))} \\ &\times e^{-\jmath\omega_c(\overbrace{\beta_{m'_f}+\beta_{m'_b}}^{C}+\beta_{m_f}+\beta_{m_b})(-t)} \\ &\times e^{-\jmath\omega_c(\overbrace{\tau_k(\theta_{m'_f})+\tau_j(\theta_{m'_b})}^{D}+\tau_i(\theta_{m_f})+\tau_j(\theta_{m_b}))} f_i(-t) \\ &+A\cdot e^{-\jmath\omega_c B}\cdot e^{-\jmath\omega_c C(-t)}\cdot e^{-\jmath\omega_c D}\cdot n'_j(-t) + e'_k(-t),\end{aligned} \tag{16}$$

where $\{m'_f, m'_b\}$ are, respectively, the forward and backward paths for the TR step, terms $\{A, B, C, D\}$ are attenuation, range, Doppler shift, and DOD/DOA expressions for TR (which are similar in nature to their conventional MIMO counterparts), and $e'_k(t)$ is additive noise. Reference [31] shows that the term $e_k(-t)$ defined as $e_k(-t) = A\exp(-\jmath\omega_c B)\exp(-\jmath\omega_c C(-t))\exp(-\jmath\omega_c D)n'_j(-t)$ $+e'_k(-t)$ closely models white Gaussian noise under minor constraints. Further, the summation term in Eq. (16) can be reorganized as a combination of two components. For the first component, $m'_f = m_f$ and $m'_b = m_b$, where the conventional MIMO signal and TR signal propagate using the same path. For the second component, $m'_f \neq m_f$ or/and $m'_b \neq m_b$, where the TR and conventional MIMO signals propagate via different paths. By exploiting the super-resolution focusing of TR, Reference [31] shows that the first component ($m'_f = m_f$ and $m'_b = m_b$), is predominant over the second component. Ignoring the second component, (16) simplifies to

$$\begin{aligned}z_k(t) = &\sum_j^{N_r} g_j \sum_i^{N_t}\sum_l^{L}\alpha^{(\mathrm{TR})}_l e^{-\jmath\omega_c 2\beta_l(-t)} \\ &e^{-\jmath\omega_c(\tau_k(\boldsymbol{\theta}_l)+2\tau_j(\boldsymbol{\theta}_l)+\tau_i(\boldsymbol{\theta}_l))} f_i(-t) + e'_k(-t),\end{aligned} \tag{17}$$

where $\alpha^{(\mathrm{TR})}_l = |\alpha_{m_f}|^2|\alpha_{m_b}|^2 e^{-\jmath\omega_c 2\left(\tau_{m_f}(0)+\tau_{m_b}(0)\right)}$. As for the conventional MIMO radar, the TR observation (17) is discretized and expressed in terms of pulses p, $(1 \le p \le N_p)$, constituting $f_i(t)$ in the vector-matrix format as

$$\begin{aligned}\mathbf{z}_{(k,p)} &= [z_k((p-1)T + 0T_s), \cdots, z_k((p-1)T + (N_s-1)T_s)]^T \\ &= \sum_l^{L}\alpha^{(\mathrm{TR})}_l d((p-1)T, 2\beta_l)\mathbf{D}(2\beta_l)\mathbf{F}(-t)\mathbf{A}(\boldsymbol{\theta}_l)\mathbf{g} + \mathbf{e}'_{k,p}(-t),\end{aligned} \tag{18}$$

where $\mathbf{A}(\boldsymbol{\theta}_l) = \begin{bmatrix} e^{-\jmath\omega_c\tau(1,1,\boldsymbol{\theta}_l)} & \cdots & e^{-\jmath\omega_c\tau(1,N_r,\boldsymbol{\theta}_l)} \\ \vdots & \ddots & \vdots \\ e^{-\jmath\omega_c\tau(N_t,1,\boldsymbol{\theta}_l)} & \cdots & e^{-\jmath\omega_c\tau(N_t,N_r,\boldsymbol{\theta}_l)} \end{bmatrix}$,

$\tau(j,i,\boldsymbol{\theta}_l) = \tau_k(\boldsymbol{\theta}_l) + 2\tau_j(\boldsymbol{\theta}_l) + \tau_i(\boldsymbol{\theta}_l)$, and $\mathbf{g} = [g_1, \cdots, g_{N_r}]^T$. Noise vector $\mathbf{e}'_{k,p}(-t)$ collects noise samples $e'_k(-t)$ for pulse p as was the case for the MIMO radar in Eq. (10).

5. THE CSTR/MIMO RADAR

The derivation of the Dantzig selector for the CSTR/MIMO radar follows the steps used for the CS/MIMO radar. Discretizing the channel into L' cells, the TR dictionary is given by

$$\begin{aligned}\mathbf{\Psi}^{(\mathrm{TR})}_{(k,p)}(\mathbf{a}) \triangleq [&d((p-1)T, 2\beta_1)\mathbf{D}(2\beta_1)\mathbf{F}(-t)\mathbf{A}(\boldsymbol{\theta}_1)\mathbf{g}, \\ &\cdots, d((p-1)T, 2\beta_{L'})\mathbf{D}(2\beta_{L'})\mathbf{F}(-t)\mathbf{A}(\boldsymbol{\theta}_{L'})\mathbf{g}].\end{aligned} \tag{19}$$

Using the dictionary $\mathbf{\Psi}^{(\mathrm{TR})}_{(k,p)}(\mathbf{a})$ and the vector of unknowns $\mathbf{s}^{(\mathrm{TR})}_{(j,p)} = [\alpha^{(\mathrm{TR})}_1, \cdots, \alpha^{(\mathrm{TR})}_{L'}]$, Eq. (18) is given by

$$\mathbf{z}_{(k,p)} = \mathbf{\Psi}^{(\mathrm{TR})}_{(k,p)}(\mathbf{a})\mathbf{s}^{(\mathrm{TR})}_{(k,p)} + \mathbf{e}'_{(k,p)} \tag{20}$$

Compressing with the $(N_c \times N_s)$ Gaussian matrix $\mathbf{\Phi}^{(\mathrm{TR})}_{(k,p)}$ gives

$$\mathbf{z}_{c(k,p)} = \mathbf{\Phi}^{(\mathrm{TR})}_{(k,p)}\mathbf{\Psi}^{(\mathrm{TR})}_{(k,p)}(\mathbf{a})\mathbf{s}^{(\mathrm{TR})}_{(k,p)} + \mathbf{e}_{(k,p)}, \tag{21}$$

where $\mathbf{e}_{(k,p)}$ is the compressed version of $\mathbf{e}'_{(k,p)}$. Organizing all TR signals in the fusion center, we get

$$\begin{aligned}\mathbf{z}_c &= \left[\mathbf{z}^T_{c(1,1)}, \cdots, \mathbf{z}^T_{c(1,N_p)}, \cdots, \mathbf{z}^T_{c(N_t,1)}, \cdots, \mathbf{z}^T_{c(N_t,N_p)}\right]^T \\ &= \mathbf{\Theta}^{(\mathrm{TR})}_{z_c}\mathbf{s}^{(TR)} + \hat{\mathbf{e}},\end{aligned} \tag{22}$$

where

$\mathbf{\Theta}^{(\mathrm{TR})}_{z_c} = \Big[\big(\mathbf{\Phi}^{(\mathrm{TR})}_{(1,1)}\mathbf{\Psi}^{(\mathrm{TR})}_{(1,1)}\big)^T \cdots, \big(\mathbf{\Phi}^{(\mathrm{TR})}_{(1,N_p)}\mathbf{\Psi}^{(\mathrm{TR})}_{(1,N_p)}\big)^T, \cdots,$

$\big(\mathbf{\Phi}^{(\mathrm{TR})}_{(N_t,1)}\mathbf{\Psi}^{(\mathrm{TR})}_{(N_t,1)}\big)^T, \cdots, \big(\mathbf{\Phi}^{(\mathrm{TR})}_{(N_t,N_p)}\mathbf{\Psi}^{(\mathrm{TR})}_{(N_t,N_p)}\big)^T\Big]^T,$

and $\hat{\mathbf{e}} = \Big[\big(\mathbf{\Phi}^{(\mathrm{TR})}_{(1,1)}\mathbf{e}_{(1,1)}\big)^T, \cdots, \big(\mathbf{\Phi}^{(\mathrm{TR})}_{(1,N_p)}\mathbf{e}_{(1,N_p)}\big)^T, \cdots,$

$\big(\mathbf{\Phi}^{(\mathrm{TR})}_{(N_t,1)}\mathbf{e}_{(N_t,1)}\big)^T, \cdots, \big(\mathbf{\Phi}^{(\mathrm{TR})}_{(N_t,N_p)}\mathbf{e}_{(N_t,N_p)}\big)^T\Big]^T.$

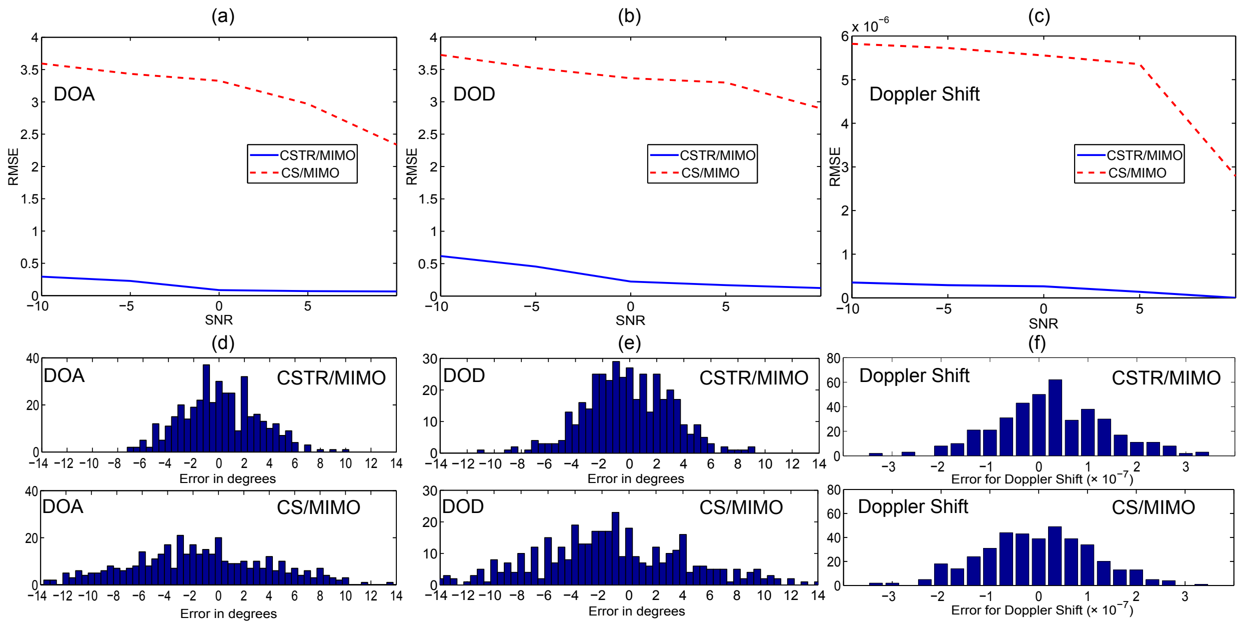

Fig. 1: Comparison between the CS/MIMO and CSTR/MIMO radars: (a)-(c) RMSE plots for the DOA (subplot (a)), DOD (subplot (b)), and Doppler shift (subplot (c)), and; (d)-(f) Error histograms at 5dB SNR for the CSTR/MIMO radar (top subplots) and CS/MIMO radar (bottom subplots). The CS/MIMO error spreads are wider in the DOA (subplot (d)), DOD (subplot (e)), and Doppler (subplot (f)) estimates.

As for the TR/MIMO radar, the fusion center in the CSTR/ MIMO radar recovers $\mathbf{s}^{(\mathrm{TR})}$ in (22) using the Dantzig selector

$$\hat{\mathbf{s}}^{(\mathrm{TR})} = \min \left\| \mathbf{s}^{(\mathrm{TR})} \right\|_1 \ \text{ s.t. } \left\| (\boldsymbol{\Theta}_{z_c}^{(\mathrm{TR})})^H (\mathbf{z}_c - \boldsymbol{\Theta}_{z_c}^{(\mathrm{TR})} \mathbf{s}^{(\mathrm{TR})}) \right\|_\infty < \mu^{(\mathrm{TR})}, \quad (23)$$

with $\mu^{(\mathrm{TR})} < \|(\boldsymbol{\Theta}_{z_c}^{(\mathrm{TR})})^H \mathbf{z}_c\|_\infty$. The selector recovers $\mathbf{s}^{(\mathrm{TR})}$ with high probability if $N_c \geq L\xi^2(\log L')^4/\mathcal{C}$, where ξ is the maximum mutual coherence between two columns of $\boldsymbol{\Theta}_{z_c}^{(\mathrm{TR})}$ and $\mathcal{C}$ is a constant.

Remarks: The paper focuses on the potential of applying TR to the CS/MIMO radar in rich multipath environments, therefore, the CSTR/MIMO vector $\mathbf{z}_{(k,p)}$ and its CS/MIMO counterpart $\mathbf{r}_{(k,p)}$ are each compressed by 12.5%. In other words, the length of $\mathbf{z}_{c(k,p)}$ (and $\mathbf{r}_{c(k,p)}$) is one eighth $(1/8)$ the length of $\mathbf{z}_{(k,p)}$ (and $\mathbf{r}_{(k,p)}$), respectively. The refocusing of the signal on the targets attributed to the TR super-resolution focusing phenomena leads us to the belief that the CSTR/MIMO radar will fare better than the TR/MIMO radar in multipath environments. Next, we demonstrate the improved performance of the CSTR/MIMO radar using Monte Carlo simulations.

6. NUMERICAL SIMULATIONS

Table 1 list the values of parameters used in our simulations. The inter-element spacing in the two transducer arrays $\{\mathcal{A}, \mathcal{B}\}$ of transducers is non-uniform to minimize the mutual coherence between the two columns of the sensing matrices $\boldsymbol{\Theta}_{r_c}$ and $\boldsymbol{\Theta}_{z_c}$ [17]. For the same reason, the probing signal $\mathbf{F}$ is chosen to be a random BPSK matrix with orthogonal columns. Our setup consists of a single target and six clutter scatterers distributed at random, i.e, $L = 7$. To quantify the performance of both the CS/MIMO and CSTR/MIMO radars, we ran Monte Carlo (MC) simulations for different SNRs ranging from -10dB to 10dB. Each MC simulation comprised 400 runs. The root mean square error (RMSE) plots for the CS/MIMO and CSTR/MIMO radars are plotted in Fig. 1(a), (b), and (c), respectively, for the DOA, DOD, and Doppler shift. In all three RMSE

Table 1: Parameters used in the Monte Carlo simulations.

Parameter	**Value**	**Comment**
N_t, N_r	24	Number of transmit/receive elements
N_s	512	Number of samples
N_c	64	Number of compressed samples
N_p	20	Number of pulses/sec
ω_c	$2\pi \times 5 \times 10^9$ rad/s	Carrier frequency
$\mathbf{F}$	$(N_s \times N_t)$	Random BPSK probing signal
$v_{m_f} = v_{m_b}$	$(300, \cdots, 400)$m/s	Velocity of forward/backwards paths with 10m/s resolution
$\theta_{m_f} = \theta_{m_b}$	$(-7°, \cdots, 7°)$	DOD & DOA with 0.5° resolution
L'	9251	Number of dictionary atoms
L	7	Number of scatterers

plots, the CS/MIMO radar has lower errors. Figs. 1(d), (e), and (f), respectively, plot the error histograms for the DOA, DOD, and Doppler shift resulting from the CSTR/MIMO radar (top subplots) and CS/MIMO radar (bottom subplots). The error spreads for the CS/MIMO radar are wider than those for the CSTR/MIMO radar verifying the superiority of the CSTR/MIMO radar.

7. CONCLUSION AND FUTURE WORKS

The paper incorporates the TR principle in the CS/MIMO radar, introduced previously in [7], for joint estimation of the DOA, DOD, and Doppler information on potential targets embedded in highly cluttered environments. The proposed CSTR/MIMO radar uses multipath constructively to focus the TR probing signals on to the targets. The CSTR/MIMO system outperforms the CS/MIMO system in our Monte Carlo simulations of a surveillance environment with a single airborne target and six scatterers introducing multipath at SNRs ranging from -10dB to 10dB. In future, we will focus on the compressibility aspects of CS in the CSTR/MIMO radars.

8. REFERENCES

[1] E. Fishler, A. Haimovich, R. Blum, L. Cimini, D. Chizhik, and R. Valenzuela, *Spatial diversity in radars: Models and detection performance*, IEEE Transaction on Signal Processing, vol. 54, pp. 823-838, Mar. 2006.

[2] J. Li, P. Stoica, and X. Zheng, *Signal synthesis and receiver design for MIMO radar imaging*, IEEE Transaction on Signal Processing, vol. 56, pp. 3959-3968, Aug. 2008.

[3] J. Li and P. Stoica, *MIMO radar with colocated antennas*, IEEE Signal Processing Magazine, vol. 24, pp. 106-114, Sept. 2007.

[4] A. Haimovich, R. Blum, and L. Cimini, *MIMO radar with widely separated antennas*, IEEE Signal Processing Magazine, vol. 25, pp. 116-129, Jan. 2008.

[5] C.Y. Chen and P.P. Vaidyanathan, *MIMO radar space-time adaptive processing using prolate spheroidal wave functions*, IEEE Transaction on Signal Processing, vol. 56, pp. 623-635, Feb. 2008.

[6] I. Bekkerman and J. Tabrikian, *Target detection and localization using MIMO radars and sonars*, IEEE Transaction on Signal Processing, vol. 54, pp. 3873-3883, Oct. 2006.

[7] Y. Yu, A.P. Petropulu, and V.H. Poor, *MIMO radar using compressive sampling*, IEEE Journal of Selected Topics in Signal Processing. vol. 4(1), pp. 146-163, 2010.

[8] CY Chen and PP Vaidyanathan, *Compressed sensing in MIMO radar*, Conference on Signals, Systems and Computers, 42nd Asilomar, pp. 41-44, 2008

[9] E.J. Candes and M.B. Wakin, *An introduction to compressive sampling*, IEEE Signal Processing Magazine, vol. 25(2), pp. 21-30, 2008

[10] E.J. Candes, *Compressive sampling*, Proceedings of the international congress of mathematicians, vol. 3, pp. 1433-1452, 2006.

[11] D.L. Donoho, *Compressed sensing*, Information Theory, IEEE Transactions on, vol. 52, pp. 1289–1306, 2006,

[12] A.C. Gurbuz, James H McClellan, and Volkan Cevher, *A compressive beamforming method*, IEEE International Conference on Acoustics, Speech and Signal Processing, ICASSP, pp. 2617-2620, 2008

[13] D. Malioutov, M. Çetin, and A.S. Willsky, *A sparse signal reconstruction perspective for source localization with sensor arrays*, IEEE Transactions on Signal Processing, vol. 53(8), pp. 3010-3022, 2005

[14] M.A. Herman and T. Strohmer, *High-resolution radar via compressed sensing*, IEEE Transactions on Signal Processing, vol. 57(6), pp. 2275-2284, 2009

[15] L. Carin, *On the relationship between compressive sensing and random sensor arrays*, IEEE Antennas and Propagation Magazine, vol. 51(5), pp. 72-81, 2009

[16] N. Wagner, Y.C. Eldar, and Zvi Friedman, *Compressed beamforming in ultrasound imaging*, IEEE Transactions on Signal Processing, vol. 60(9), pp. 4643-4657, 2012

[17] M. Rossi, A. Haimovich, and Y.C. Eldar, *Spatial compressive sensing for MIMO radar*, IEEE Transactions on Signal Processing, vol. 62(2), pp. 419-430, 2014

[18] Y.C. Eldar and G. Kutyniok, *Compressed sensing: theory and applications*, Cambridge University Press, 2012

[19] A. Hassanien and S.A. Vorobyov, *Transmit/receive beamforming for mimo radar with collocated antennas*, IEEE International Conference on Acoustics, Speech, and Signal Processing (ICASSP), pp. 2089-2092, 2009.

[20] F. Foroozan and A. Asif, *Information theoretic bounds for Angle-Doppler estimation in time reversal MIMO communication*, IEEE Global Communications Conference (GLOBECOM), pp. 3975-3981, 2012

[21] J.E. Candès and T. Tao, *The Dantzig selector: Statistical estimation when p is much larger than n*, The Annals of Statistics, JSTOR, pp. 2313-2351, 2007.

[22] P. Blomgren, G.C. Papanicolaou, and H. Zhao, *Super-resolution in time-reversal acoustics*, Journal of the Acoustical Society of America, vol. 111, 230-248, 2001.

[23] C. Tsogka and G. C. Papanicolaou, *Time reversal through a solid-liquid interface and super-resolution*, Inverse problems, vol. 18, no. 6, pp. 1639-1657, 2002.

[24] M. Fink, *Time reversal of ultrasonic fields – Part I: Basic principles*, IEEE Transactions on Ultrasonics, Ferroelectrics and Frequency Control, vol. 39, no. 5, pp. 555-566, Sep. 1992.

[25] Y. Jin and J. Moura, *Time-reversal detection using antenna arrays*, IEEE Transactions on Signal Processing, vol. 57, no. 4, pp. 1396-1414, Apr. 2009.

[26] Y. Jin, J. Moura, and N. Donoughue, *Time reversal in multiple-input multiple-output radar*, IEEE Journal of Special Topics in Signal Processing, vol. 4, no. 1, pp. 210-225, Feb. 2010.

[27] F. Foroozan and A. Asif, *Time reversal based active array source localization*, IEEE Transactions on Signal Processing, vol. 59, no. 6, pp. 2655-2668, Jun. 2011.

[28] F. Foroozan and A. Asif, *Cramer-Rao bound for time reversal active array direction of arrival estimators in multipath environments*, IEEE International Conference on Acoustics, Speech, and Signal Processing (ICASSP), pp. 2646-2649, Mar. 2010.

[29] F. Foroozan, A. Asif, Y. Jin, and J. Moura, *Direction finding algorithms for time reversal MIMO radars*, IEEE Statistical Signal Processing Workshop (SSP), pp. 433-437, 2011.

[30] F. Foroozan and A. Asif, *Time reversal MIMO radars for estimation of velocity and direction*, IEEE Statistical Signal Processing Workshop (SSP), pp. 860-863, 2012.

[31] F. Foroozan, A.Asif, and R. Boyer, *Angular Resolution Limit for The Time Reversal MIMO Radar*, IEEE International Conference on Acoustics, Speech, and Signal Processing (ICASSP), pp. 4125-4129, 2013.

[32] M. Sajjadieh and A. Asif, *Uniform rectangular time reversal arrays: Joint azimuth and elevation estimation*, IEEE Statistical Signal Processing Workshop (SSP), pp. 89-92, 2012.